Biophysical Journal Volume 68 April 1995 1583–1591

Stark Effect Spectroscopy of Tryptophan

Daniel W. Pierce and Steven G. Boxer
Department of Chemistry, Stanford University, Stanford, California 94305 USA

ABSTRACT The change in permanent dipole moment ($|\Delta\vec{\mu}|$) for the transition from the ^1L_a state to the ground state of tryptophan is the key photophysical parameter for the interpretation of tryptophan fluorescence spectra in terms of static and dynamic dielectric properties of the surrounding medium. We report measurement of this parameter by means of electric field effect (Stark) spectroscopy for *N*-acetyl-L-tryptophanamide (NATA) in two solvents, the single tryptophan containing peptide melittin, and 5-methoxytryptophan. The values ranged from 5.9 to 6.2 ± 0.4 Debye/*f* for NATA and melittin, where *f* represents the local field correction. The ^1L_b $|\Delta\vec{\mu}|$ was much smaller. Application of Stark spectroscopy to these chromophores required decomposition of the near-UV absorption into the ^1L_a and ^1L_b bands by measurement of the fluorescence excitation anisotropy spectrum and represents an extension of the method to systems where band overlap would normally preclude quantitative analysis of the Stark spectrum. The results obtained for 5-methoxytryptophan point out limitations of this method of spectral decomposition. The relevance of these results to the interpretation of steady-state and time-resolved spectroscopy of tryptophan is discussed.

INTRODUCTION

Measurement of steady-state and time-resolved fluorescence of tryptophan is widely used for characterization of peptides and proteins, and results are routinely interpreted in terms of the static polarity and heterogeneity of the local environment as well as the dynamic properties of the environment and the emitting residue (Beecham and Brand, 1985). The key photophysical parameter for the interpretation of fluorescence in terms of local polarity is the change in permanent dipole moment ($|\Delta\vec{\mu}|$) on absorption. The classical method for measuring this quantity is to measure the fluorescence spectrum in a series of solvents of known polarity. The difference dipole is given by the Ooshika-Lippert-Mataga relation (Lippert, 1957):

$$\langle\Delta\nu\rangle = \frac{2\,(\vec{\mu}_e - \vec{\mu}_g)^2}{ha^3}\left(\frac{\epsilon_0 - 1}{2\epsilon_0 + 1} - \frac{n^2 - 1}{2n^2 + 1}\right) \qquad (1)$$

where $\langle\Delta\nu\rangle \equiv \langle\Delta\nu_A\rangle - \langle\Delta\nu_F\rangle$, and $\langle\Delta\nu_A\rangle$ and $\langle\Delta\nu_F\rangle$ are the shifts of the 0–0 absorption and fluorescence transition energies, respectively, due to electrostatic interactions with the medium. These shifts are measured relative to the values obtained in a nonpolar solvent. The quantities $\vec{\mu}_e$ and $\vec{\mu}_g$ are the excited- and ground-state permanent dipole moments, and $\Delta\vec{\mu} = \vec{\mu}_e - \vec{\mu}_g$. ϵ_0 is the static dielectric constant, n is the refractive index, a is the cavity radius of the solvent cavity (typically assumed to be spherical) required to accommodate the chromophore, and h is Planck's constant. This equation remains extremely useful but suffers from the same shortcomings as all relations based on a continuum dielectric model of a solvent: all perturbations due to specific interactions between solute and solvent (i.e., ground- or excited-state complex formation) and to the finite size of the solvent molecules are ignored. Such effects will adversely impact the accuracy of the determination of $|\Delta\vec{\mu}|$. In addition, $\vec{\mu}_e$ is assumed to be the same in the Franck-Condon excited state and the relaxed emitting state, and obtaining reliable absorption and fluorescence spectra of dipolar or charged molecules in a truly nonpolar reference solvent can be challenging because of limited solubility and aggregation. A better method, in principle, is to measure the effect of an externally applied electric field on the electronic transition (the Stark effect; Liptay, 1976). The electric field changes the wavelength-dependent molar absorption coefficient in a manner dependent on $|\Delta\vec{\mu}|$, the change in the average polarizability ($Tr\Delta\alpha$), and the internal angle ζ between the transition moment $\vec{m}$ and $\Delta\vec{\mu}$.

Here we report the results of Stark effect and fluorescence excitation anisotropy studies at low temperature (77–85 K) on *N*-acetyl-L-tryptophanamide (NATA) in ethanol (EtOH) or 50% v/v glycerol/water glass, melittin in 50% glycerol/water, and 5-methoxytryptophan in EtOH. These molecules were selected to examine the sensitivity of the spectra to different environments and to chemical substitution.

The near-UV absorption of tryptophan is believed to consist of two nearly totally overlapping π–π^* transitions, labeled ^1L_a and ^1L_b in the Platt notation (Valeur and Weber, 1977). The formalism for the analysis of Stark spectra developed by Liptay (1976) rests on the assumption that the absorption lineshape is that of a single, isolated electronic transition with wavelength-independent electrooptic properties. This assumption is necessary because the Stark spectrum is expressed in terms of sums of derivatives of the absorption lineshape. However, there is no fundamental obstacle to analysis of the Stark spectrum of overlapping transitions as long as there is some means of decomposing the total absorption into its constituent parts. In the case of

Received for publication 28 July 1994 and in final form 10 January 1995.
Address reprint requests to Dr. Steven G. Boxer, Department of Chemistry, Stanford University, Stanford, CA 94305-5080. Tel.: 415-723-4482; Fax: 415-723-4817; E-mail: sboxer@leland.stanford.edu.

0006-3495/95/04/1583/09 $2.00

tryptophan, the observation that the fluorescence originates solely from ^1L_a and the near orthogonality of the ^1L_a and ^1L_b transition moment directions provides a means for accomplishing such decomposition, performed originally by Valeur and Weber (1977). The emission anisotropy at differing excitation wavelengths is measured and interpreted in terms of the fractional absorption accounted for by each transition moment at each excitation wavelength. 5-Methoxytryptophan was selected because substitution of electron-withdrawing moieties at position 5 is thought to selectively lower the energy of the ^1L_b transition and switch the order of 0–0 energies in both absorption and fluorescence without perturbation of ^1L_a, and previous work has indicated that this is the only methoxy derivative that retains orthogonality of the transition moments (Eftink et al., 1990).

MATERIALS AND METHODS

NATA was a gift of David J. Lockhart. Melittin and 5-methoxytryptophan were purchased from Sigma Chemical Co. (St. Louis, MO) and used without further purification. The glycerol was Mallinkrodt AR grade and the EtOH was Aldrich spectrophotometric grade.

Stark and absorption spectra

The Stark apparatus used in these experiments has been described elsewhere (Boxer, 1993). Light from a 450-W Xe arc lamp (Spex) was dispersed through a Spex Minimate ¼-m monochromator (0.9-nm resolution), collimated, passed through an air-spaced Glan-Taylor polarizer and a strain-free quartz optical dewar containing the sample immersed in liquid nitrogen, and detected by a photomultiplier tube on which the resistor network had been altered so as to bypass the last few dynodes and decrease the noise. The photomultiplier signal was converted to a voltage and amplified using a home-built converter/amplifier and fed into a lock-in amplifier (Stanford Research Systems SR530). Samples consisted of 15 μl of solution between two quartz slides held apart by a 25-μm Kapton spacer. The quartz slides were rendered conductive by means of an evaporated layer of nickel ~7.5 nm thick, corresponding to a transmittance of about 50% per slide in the near UV and visible and a resistance of not more than 1000 Ω. 400-Hz sinusoidal AC electric fields with peak-to-peak voltages from 2 to 4.5 kV were produced by a custom-built power supply and applied to the sample. The raw data are the intensity of the signal at the photomultiplier, $I(\nu)$, and the amplitude of its modulation at twice the field frequency, $\Delta I(\nu)$. The Stark spectrum is $\Delta I(\nu)/(I(\nu)-k)$, where k is a constant baseline voltage from the amplifier. Because the electric field modulation is small ($<1 \times 10^{-4}$ of I), the Stark spectrum may be identified with the field-induced change in absorption $\Delta G(\nu)$ without significant loss of accuracy.

Low-temperature absorption spectra of samples versus air were recorded at 1 nm resolution on a Varian 2300 spectrophotometer in the same optical dewar and on the same samples used for the Stark experiments and were baseline corrected by means of a blank sample. Absorption spectra recorded at 0.5 nm resolution were identical within the signal-to-noise obtained. Peak optical densities ranged from approximately 0.1 to 0.4 absorbance units. Sample thicknesses were determined by measurement of interference fringe spacings in the absorption spectrum of the unfilled sample cell at room temperature between 500 and 600 nm. Wavelength calibration of the absorption, Stark, and fluorescence excitation spectra (see below) was accomplished by measurement of the apparent position of the 361.0 nm absorbance of a Holmium filter on each apparatus.

Fluorescence excitation spectra

Polarized fluorescence spectra (1.8 nm resolution) and fluorescence excitation spectra (0.9 nm resolution, 14-nm emission bandpass) were recorded on a modified Spex Fluorolog equipped with double monochromators for selection of the excitation wavelength and dispersal of the fluorescence. The excitation source was a 450-W Xe arc lamp, and the detector a Hamamatsu R955P photomultiplier in a cooled housing in photon-counting mode. An optical dewar was installed in the sample compartment and cooled to 85 K with a stream of cold N_2 gas. It was found that use of liquid N_2 caused an unacceptable degree of depolarization of the excitation and emission due to scattering caused by snow, bubbles, and schlieren; Stark spectra taken at 85 K in a gas-cooled dewar were indistinguishable from spectra taken at 77 K immersed in liquid N_2. Scattering was minimized in the Stark experiments by blowing He over the surface of the liquid N_2, thereby eliminating bubbles. This source of interference is less of a problem in the Stark experiments because field modulation and lock-in detection sharply reduces its contribution to the measured signal. It was necessary to use thin (75-μm) samples in these experiments because 50% glycerol/water does not form clear glasses in samples more than 75 μm thick, and it was therefore necessary to collect fluorescence from the front face of the sample. Two linear dichroic polarizers were installed just before and after the sample in the optical path, as the Glan-Thompson polarizers supplied with the instrument were found to absorb and fluoresce in the near-UV and obstructed an unacceptable portion of the beam. Modification of the excitation monochromator by installation of masks in front of two of the spherical mirrors was necessary to eliminate artifacts due to unwanted propagation of the zero-order reflection off the grating surfaces back along the optical path. Fluorescence spectra were corrected by means of a standard lamp, and fluorescence excitation anisotropy spectra were corrected by reference to an unpolarized fluorescence source (NATA or anthracene in methanol at room temperature), as this was judged less prone to source geometry artifacts than the standard lamp. Fluctuations in lamp intensity were corrected for by use of a rhodamine quantum counter solution. Because the optical paths to the sample and quantum counter solution differ, it is necessary to correct the quantum counter correction to obtain unbiased fluorescence excitation spectra, although these differences ratio out in the fluorescence excitation

anisotropy spectrum. For the front-face detection geometry used, such a correction contains systematic errors due to rhodamine monomer emission that render the excitation spectrum useless for quantitative comparison with the absorption spectrum. For this reason we do not report the fluorescence excitation spectra.

Theory and methods of data analysis

The Stark spectrum recorded at twice the field modulation frequency of a single electronic transition can often be described as a linear combination of appropriately weighted derivatives of the absorption spectrum $G(\nu)$ (Liptay, 1976):

$$\frac{\Delta G(\nu,\chi)}{\nu} = \left\{ A(\chi)\left(\frac{G(\nu)}{\nu}\right) + \frac{B(\chi)}{15h}\frac{\partial}{\partial\nu}\left(\frac{G(\nu)}{\nu}\right) + \frac{C(\chi)}{30h^2}\frac{\partial^2}{\partial\nu^2}\left(\frac{G(\nu)}{\nu}\right)\right\} \cdot \vec{\mathbf{F}}_{\text{int}}^2 \tag{2}$$

where h is Planck's constant, χ is the experimental angle between the external field $\vec{\mathbf{F}}_{\text{ext}}$ and the electric polarization vector of the linearly polarized light used to probe the sample. The internal and external fields differ slightly due to the Lorentz local field correction (see below). A_χ, B_χ, and C_χ are fully described elsewhere (Liptay, 1976; Oh et al., 1991). Roughly, A_χ depends on the transition moment polarizability and hyperpolarizability, B_χ on the change in polarizability $\Delta\vec{\alpha}$ and C_χ on $\Delta\vec{\mu}$ and the internal angle ζ between the transition moment $\vec{m}$ and $\Delta\vec{\mu}$. ζ is determined by the χ-dependence of C_χ. In the case of overlapping transitions, the Stark spectrum is to be regarded as a sum of the spectra of the underlying transitions with independent coefficients A_χ, B_χ, and C_χ for each transition:

$$\frac{\Delta G(\nu,\chi)}{\nu} = \sum_i \frac{\Delta g_i(\nu,\chi)}{\nu} \tag{3}$$

where $\Delta g_1(\nu)/\nu$ is the (unobservable) Stark spectrum of each transition with lineshape $g_1(\nu)$.

The fluorescence excitation and emission anisotropy spectra are given by (Lakowicz, 1983):

$$r(\nu) = \frac{I_\parallel(\nu) - k(\nu)I_\perp(\nu)}{I_\parallel(\nu) + 2k(\nu)I_\perp(\nu)} \tag{4}$$

where $k(\nu)$ corrects for the differential sensitivity of the detection apparatus at the emission wavenumber detected, and ν is the wavenumber of absorption or emission. For a single electronic transition, $r(\nu)$ is constant if the transition moment direction is not affected by vibronic coupling or inhomogeneous effects. For the case where two states absorb, but only one emits, the absorption spectrum can be decomposed according to Valeur and Weber (1977):

$$g_1(\nu) = G(\nu)\left[\frac{r_{\text{ex}}(\nu) - r_2}{r_1 - r_2}\right]; \qquad g_2(\nu) = G(\nu) - g_1(\nu) \tag{5}$$

where $g_1(\nu)$ is the absorption spectrum of the emitting state, and r_1 and r_2 are the emission anisotropies that would be observed were it possible to excite only state 1 or 2, respectively. Two assumptions must be made to obtain this equation: 1) the limiting anisotropies r_1 and r_2 must be wavelength independent, i.e., vibronic coupling or other effects must not perturb the transition moment directions; and 2) the quantum yield for excitation into state 1 and emission from state 1 must be identical to the quantum yield for excitation into state 2 and emission from state 1. This requirement is met if the quantum yield for internal conversion of state 2 to state 1 is unity. If the quantum yield for emission is excitation wavelength dependent, such dependence must be identical for both states.

If the transition moments for absorption and emission for state 1 and the transition moment for absorption for state 2 are constrained to lie in a plane, the angle Θ_{12} between the transition moments for absorption is given by:

$$\Theta_{12} = \cos^{-1}\sqrt{\frac{r_1 + r_2 - \frac{1}{5}}{2r_1 - \frac{1}{5}}} \tag{6}$$

The work of Valeur and Weber (1977) contains the equations necessary to derive this expression.

The basic approach taken in this work is to simultaneously fit four different experimental spectra: the Stark spectrum at two values of the angle χ the absorption spectrum, and the fluorescence excitation anisotropy spectrum. Each absorption spectrum is represented by an arbitrary number of non-normalized gaussians:

$$g_i(\nu) = \sum_j \Phi_j \exp\left(-\left(\frac{\nu - \nu_j}{\sigma_j}\right)^2\right) \tag{7}$$

The explicit fitting functions are then:

$$\frac{\Delta G(\nu,\chi)}{\nu} = \sum_i \left\{ A_{i,\chi}\left(\frac{g_i(\nu)}{\nu}\right) + \frac{B_{i,\chi}}{15h}\frac{\partial}{\partial\nu}\left(\frac{g_i(\nu)}{\nu}\right) + \frac{C_{i,\chi}}{30h^2}\frac{\partial^2}{\partial\nu^2}\left(\frac{g_i(\nu)}{\nu}\right)\right\} \tag{8}$$

$$G(\nu,\chi) = \sum_i g_i(\nu) \tag{9}$$

and

$$r_{\text{ex}}(\nu) = \frac{r_1 g_1(\nu) + r_2 g_2(\nu)}{G(\nu)} \tag{10}$$

where the subscript i runs from 1 to 2 in Eqs. 8 and 9. Fits were performed using the Levenburg-Marquardt and Simplex algorithms (Press et al., 1992). All parameters, with the exception of the $A_{i,\chi}$, were allowed to vary in the final minimizations. The $A_{i,\chi}$ were constrained to be zero. $A_{i,\chi}$ principally gives the magnitude of the transition moment polarizability and hyperpolarizability. In our experience this term makes a negligible contribution to the total Stark signal for small planar aromatic molecules, and its inclusion here would have made the fitting procedure less well determined.

The electrooptic parameters determined from the fits are expressed in terms of the local field correction f to separate the experimental uncertainties associated with the measurement from uncertainties in the value of f. This factor corrects for the change in electric field strength inside a cavity (in this case, the cavity containing the chromophore) with dielectric properties different from those of the bulk. It depends on the shape of the cavity and the contrast in dielectric constant between the medium and the material in the cavity. For a spherical cavity, the Onsager form is most appropriate for these samples (Hill et al., 1969; Böttcher, 1973):

$$f = \frac{3\epsilon_2}{2\epsilon_2 + \epsilon_1} \tag{11}$$

where ϵ_1 is the dielectric constant of the contents of the cavity, and ϵ_2 is the dielectric constant of the solvent. If $\epsilon_1 < \epsilon_2$, f lies between 1.0 and 1.5. Taking the dielectric constants of frozen 50% glycerol/water or EtOH as 3.5 and the dielectric constant of the chromophore as 2.0 (from the square of the optical index of typical small aromatic molecules), $f \cong 1.2$. For a nonspherical cavity this value may increase. Because ϵ_1 and the cavity geometry are only approximately known and this relation is based on a continuum model of the solvent, the parameters are expressed in terms of f.

RESULTS

Fits and parameters for NATA, melittin, and 5-methoxytryptophan

Fig. 1 shows the total absorption and Stark spectra and the ^1L_a and ^1L_b parts of each for NATA in 50% glycerol/H_2O. The model function for the total absorption is the sum of the ^1L_a and ^1L_b absorption spectra. The ^1L_a and ^1L_b Stark lineshapes are the sum of the first and second derivative contributions of the corresponding absorption. The Stark spectrum is dominated by the ^1L_a part over most of the region analyzed, and the ^1L_a Stark lineshape is in turn similar to the second derivative of the ^1L_a absorption. The ^1L_b Stark lineshape is composed of more or less equal parts of the second derivative and the negative first derivative of the ^1L_b absorption. This reflects the much larger $|\Delta\vec{\mu}|$ for the ^1L_a transition. The fluorescence excitation anisotropy spectrum and the Stark spectrum at $\chi = 50°$ are not shown in Fig. 1, but were included in the least-squares minimization that generates the fits to the data as described above. All the data and fits (except for the Stark spectra at $\chi = 50°$) for NATA in 50% glycerol/water, NATA in EtOH, and melittin in 50% glycerol/water are presented in a more compact format in Figs. 2 (absorption and fluorescence excitation anisotropy spectra) and 3 (Stark effect spectra taken with $\chi = 90°$). Stark spectra at $\chi = 50°$ had a similar overall lineshape but differed in detail. Decomposed absorption spectra for these three samples are given in Fig. 4. These latter absorption spectra are model functions constrained by simultaneous fitting to two Stark spectra, the absorption spectrum, and the fluorescence excitation anisotropy spectrum. The absorption and Stark spectra and fits for 5-methoxytryptophan are given in Fig. 5. As described below, these spectra were analyzed under the assumption that all the oscillator strength in the lowest energy vibronic band comes from the ^1L_b transition.

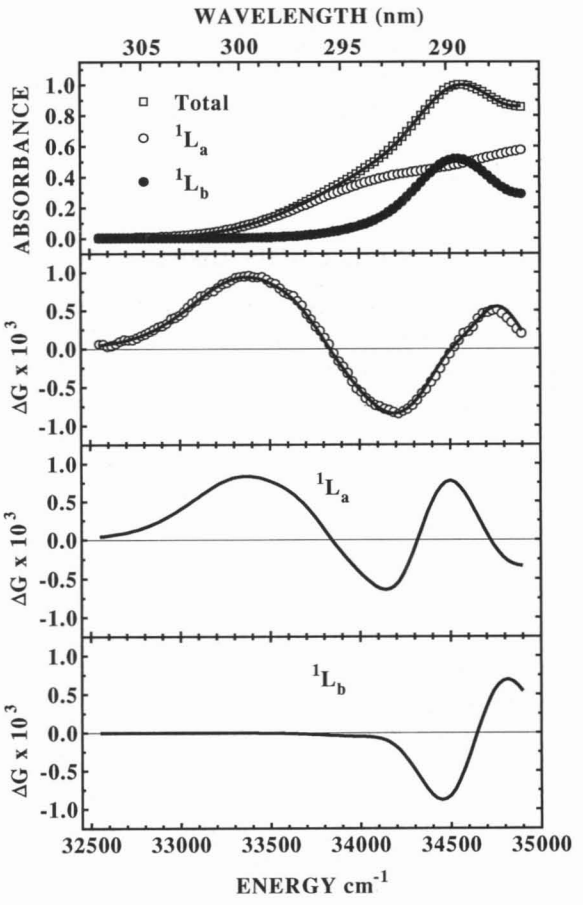

FIGURE 1 Absorption and Stark spectra and their ^1L_a and ^1L_b components for NATA in 50% glycerol/H_2O glass at 77 K. The top panel shows the total absorption spectrum and its ^1L_a and ^1L_b components derived from simultaneous fitting of the absorption, fluorescence excitation anisotropy, and Stark spectra. The absorption spectrum has been normalized to an absorbance of 1 at the absorption maximum. The peak absorbance of the samples was ~0.25. The solid line through the total absorption is the fit to the data, and is the sum of the ^1L_a and ^1L_b absorption spectra. The second panel shows the total Stark spectrum (○) at $\chi = 90°$ and fit (——). The Stark spectrum has been normalized to an absorbance of 1 at the absorption maximum and to an external field of 1×10^6 V/cm. The external field applied to the samples was $\sim 7 \times 10^5$ V/cm. The third and fourth panels show the ^1L_a and ^1L_b contributions to the Stark spectrum, respectively. These lineshapes are the sum of the first and second derivative components of the corresponding absorption. The fit to the total Stark spectrum in the second panel is the sum of the lineshapes in the third and fourth panels.

The photophysical properties calculated from the parameters used to fit the Stark spectra for all four types of samples are given in Table 1. All types of spectra for all samples were reproducible, and errors are the standard deviations of independent data sets. Some of the fit parameters were not reproducible even though the data appeared identical within the signal-to-noise ratio obtained; these parameters were ill determined because they did not give rise to a unique feature in the data. Such parameters include the polarizability change of the ^1L_a and ^1L_b transitions and the internal angle ζ between

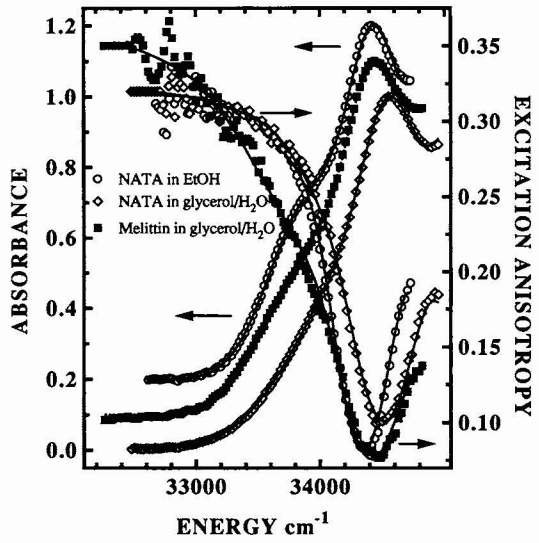

FIGURE 2 Electronic absorption and fluorescence excitation anisotropy spectra of NATA in EtOH, NATA in 50% glycerol/water, and melittin in 50% glycerol/water. The absorption spectra were recorded at 77 K and the fluorescence excitation anisotropy at 85 K (see text). Peak optical densities ranged from 0.4 for NATA in EtOH to 0.1 for melittin. The absorption spectra have been normalized to an absorbance of 1 at the absorption maximum and offset vertically for presentation. Data are represented by symbols, and the corresponding fits by solid lines.

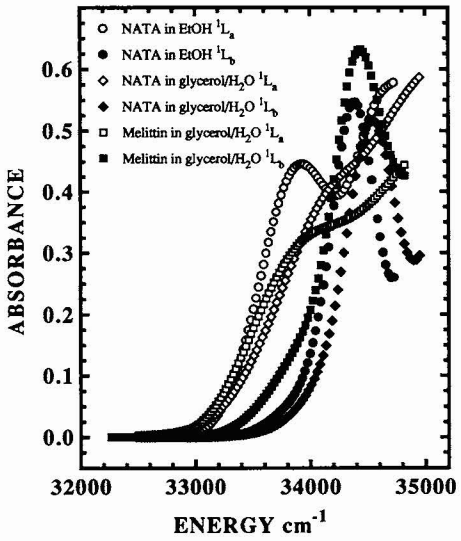

FIGURE 4 Decomposed absorption spectra showing the ^1L_a and ^1L_b lineshapes for the samples of Fig. 2. The sum of the ^1L_a and ^1L_b lineshape for each sample is the model function for the corresponding total absorption in Fig. 2.

$\Delta\vec{\mu}$ and the ^1L_b transition dipole, and these are omitted from Table 1. The limiting anisotropies were free parameters in the fit. The internal angle Θ_{ba} was calculated from Eq. 6.

The case of 5-methoxytryptophan: limitations of the absorption decomposition

The absorption and excitation anisotropy spectra for 5-methoxytryptophan are shown in Fig. 6. It is instructive to examine the qualitative features of these spectra. Consistent with the identification of the lowest energy transition in this molecule as ^1L_b, well-resolved vibronic bands are observed (Eftink et al., 1990). Vibronic structure is also apparent in the excitation anisotropy spectrum, and manifests itself as a rapid decrease in $r_{ex}(\nu)$ across each absorption peak with a flatter region between each peak. This pattern may be discerned over at least five resolved vibronic bands. If the decrease in $r_{ex}(\nu)$ were solely a consequence of increasing ^1L_a

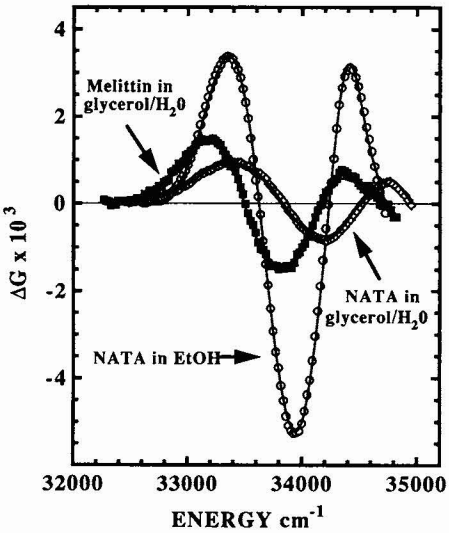

FIGURE 3 Stark effect spectra at $\chi = 90°$ corresponding to the samples of Fig. 2. Field strengths were in the range of 4×10^5 V/cm for samples in 50% glycerol/water and 7×10^3 V/cm for samples in EtOH. The data have been normalized to an absorbance of 1 at the absorption maximum and to an external field of 1×10^6 V/cm. Solid lines are fits to the data.

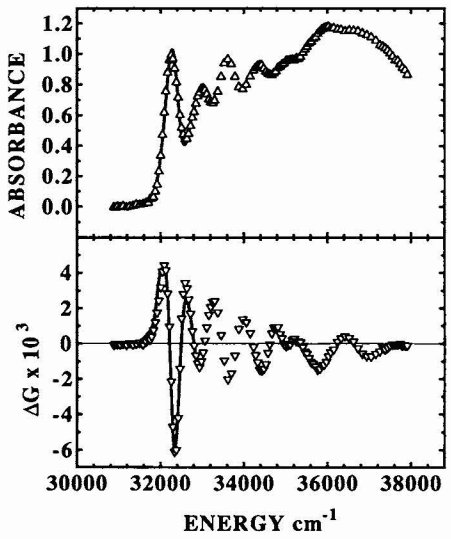

FIGURE 5 Absorption ($\triangle$) and Stark effect (∇) spectra for 5-methoxytryptophan at 77 K in EtOH. Data have been normalized to an absorbance of 1 at the absorption maximum within the range of the fit and to a field of 1×10^6 V/cm. The peak absorbance of the samples was ~0.05, and the external field $\sim 7 \times 10^5$. Fits to the data are indicated by bold lines and were performed only over the lowest energy absorption maximum (see text). This lowest energy feature is fit as for an isolated electronic transition, and the fluorescence excitation anisotropy spectrum is not included in the fits in any way.

TABLE 1 Electrooptic parameters derived from Stark spectra

	NATA in EtOH	NATA in 50% glycerol/water	Melittin	5-methoxytryptophan
$^1L_a \lvert\Delta\bar{\mu}\rvert$	5.9 ± 0.3 D/*f*	5.9 ± 0.4 D/*f*	6.2 ± 0.3 D/*f*	N/A
$^1L_b \lvert\Delta\bar{\mu}\rvert$	1.3 ± 0.3 D/*f*	1.5 ± 0.3 D/*f*	1.1 ± 0.3 D/*f*	1.7 ± 0.2 D/*f*
$^1L_a\ \zeta$	58 ± 10°	69 ± 10°	82 ± 10°	N/A
$^1L_b\ \zeta$	N/A	N/A	N/A	51 ± 5°
$^1L_a\ r_0$	0.32 ± 0.02	0.32 ± 0.02	0.35 ± 0.02	N/A
$^1L_b\ r_0$	−0.11 ± 0.02	−0.10 ± 0.02	−0.09 ± 0.02	0.33 ± 0.02
Θ_{ba}	81 ± 9°	78 + 12, −8°	70 + 20, −8°	N/A

absorption, it would be necessary to assert that all the vibronic maxima of the ^1L_a absorption correspond to those of the ^1L_b absorption to explain the structure in $r_{ex}(\nu)$. A more plausible explanation is the breakdown of assumption 1 for the absorption decomposition (see above): the limiting anisotropy for excitation into different vibronic bands of ^1L_b is not constant, but exhibits a decrease with increasing wavenumber. The fluorescence spectrum of 5-methoxytryptophan also exhibits vibronic structure (Fig. 7), but the fluorescence anisotropy spectrum does not reveal any related structure. Two explanations may be advanced to explain these observations. Absorption and fluorescence are in many respects mirror-image processes, but upon excitation vibronic coupling will mix the first excited state with other states, whereas in emission from a thermalized excited state it is the ground state that is mixed (Albrecht, 1961; Mathies, 1974; Boxer et al., 1982). For this reason, transition moment directions for vibronic bands on emission and excitation need not change in a parallel fashion. A clear example of vibronic coupling leading to rotation of the transition moment in emission is provided by the phosphorescence of 5-methoxytryptophan (Fig. 7). The pattern observed in the fluorescence excitation anisotropy spectrum is consistent with an unresolved progression in a low-frequency (probably solvent) mode leading to rotation of the transition moment across each absorption maximum, and a similar progression in an ~800 cm^{-1} mode accounting for the decrease in average anisotropy of each peak with increasing energy (Albrecht, 1961). Alternatively, we note that excitation of any transition other than the 0–0 involves deposition of vibrational energy into the molecule and shortly thereafter into its surroundings. The second resolved maximum in the 5-methoxytryptophan absorption spectrum is almost 800 cm^{-1} above the first, corresponding to a temperature of >1150 K. Although this energy will rapidly flow into a large number of low-frequency vibrational modes, perhaps enough local heating occurs so that small rotations of the molecule may occur. An analogous process could occur on emission, but by the time a vibrationally hot ground state is created the photon is gone and any rotation of the ground-state molecule will not be observed.

In either case, the validity of the absorption decomposition given by Eq. 4 must be called into question if such decomposition is carried out over multiple vibronic maxima of ei-

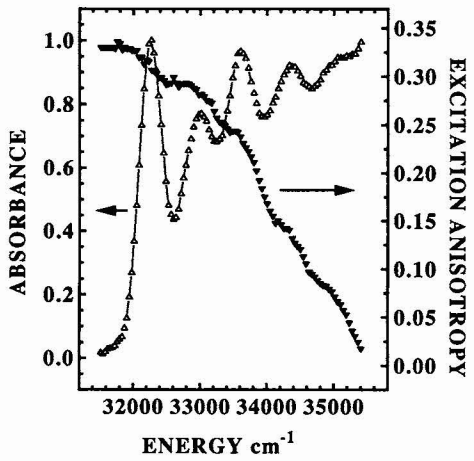

FIGURE 6 Absorption (△) and fluorescence excitation anisotropy (▽) spectra for 5-methoxytryptophan at 77 K in EtOH. The absorption data is identical to that in Fig. 5 except that a smaller range of data is shown. Solid lines do not show fits in this figure.

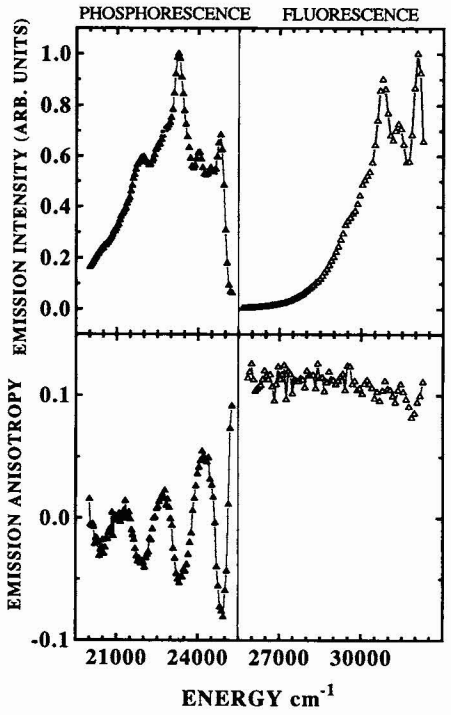

FIGURE 7 5-Methoxytryptophan singlet (△) and triplet (▲) emission and emission anisotropy spectra. The fluorescence and phosphorescence spectra have been independently scaled to a peak intensity of 1. The spectra have been corrected for the wavelength and polarization-dependent efficiency of the detection apparatus.

ther transition. For 5-methoxytryptophan, there does not appear to be a clear-cut means of identifying the onset of ^1L_a absorption from $r_{ex}(\nu)$, so we analyze the Stark spectrum of the first vibronic band in the normal manner for an isolated electronic transition. For NATA and melittin, the excitation anisotropy spectra observed are more plausibly attributed to overlapping electronic transitions. To avoid running afoul of assumption 1, we restrict our analysis of the Stark spectra of these molecules to the region containing the first vibronic band of each transition (32,000–35,000 cm^{-1}).

DISCUSSION

Comparison with solvent-dependence data

Mataga and co-workers (1964) estimated $|\Delta\vec{\mu}|$ for the ^1L_a state of indole to be 5 Debye (D) on the basis of the solvent dependence of the emission spectrum, and Gladchenko and Pikulik (1967) estimated $|\vec{\mu}_e|$ to be 5.6 D based on the temperature dependence of absorption and emission spectra. These results were called into question by Walker et al. (1967), who interpreted at least part of the solvent dependence to exciplex formation in protic solvents. Lami and Glasser (1985) undertook a more contemporary and detailed study that resolved several points of confusion in the literature. First, they demonstrated that the identity of the emitting state depends on solvent polarity for indole and several derivatives, which presents a clear problem in the interpretation of solvent-dependent emission data. Second, evidence for ground-state complex formation in all polar solvents tested leading to large shifts in the ^1L_a energy was obtained. Third, solvent effects on absorption and emission were separately evaluated. However, ground-state complex formation precluded independent determination of $|\Delta\vec{\mu}|$ for ^1L_a absorption and emission, so the assumption of no change in $\vec{\mu}_e$ on relaxation of the Franck-Condon excited state still had to be made. Under this assumption, $|\vec{\mu}_e|$ for the ^1L_a state of 3-methylindole was found to be 5.32 D, and that of the ^1L_b state of 5-methoxyindole 2.69 D. The corresponding ground-state values were 2.10 and 2.0 D, leading to $|\Delta\vec{\mu}|$ values of 3.22 and 1.69 D, respectively. This value for the ^1L_a $|\Delta\vec{\mu}|$ is smaller than that obtained in this work. The difference is too large to be accounted for by any plausible estimate of the local field correction, and must therefore be ascribed to limitations in the accuracy of one or both of the methods being compared.

Comparison with electronic structure calculations

Callis (1991) performed extensive semiempirical molecular orbital calculations on indole and was able to reproduce many experimentally observed features. Calculated ^1L_a $|\vec{\mu}_e|$ values ranged from 3.22 to 7.07 D but were generally about 5 D. A gas-phase value for $|\Delta\vec{\mu}|$ of 5.7 D for 3-methylindole is also reported by Muiño et al. (1992). However, the relevance of gas-phase calculations to condensed-phase measurements is qualitative at best. Condensed-phase molecular dynamics coupled with similar electronic structure calculations (Muiño et al., 1992) indicate an even larger value for the ^1L_a dipole. Chabalowski et al. (1993) performed *ab initio* calculations on indole including optimization of excited-state geometries and the effects of a reaction field. They found ^1L_a and ^1L_b $|\vec{\mu}_e|$ values of 6.74 and 3.17, respectively, and a $|\vec{\mu}_g|$ of 2.94 D after two iterations at the ground-state geometry and reaction field, although the convergence of the calculation after this number of iterations is unknown. However, the corresponding values for the fluorescence transition at the excited-state geometry and reaction field were 10.4, 4.72, and 5.41 D, respectively. Levy and co-workers have performed extensive vacuum and condensed phase *ab initio* electronic structure calculations with great attention to the effects of the solvent field on the properties of electronic states (Levy et al., 1991; Westbrook et al., 1992). The change in dipole moment on excitation to the ^1L_a state predicted by their work is 3.1 D. This value represents an ensemble average over many configurations of solvent. The range of values of $|\vec{\mu}_e|$ for the configurations sampled was 2.4 to 9.0 D (K. Krogh-Jespersen, personal communication), and the excited-state dipole moment was found to increase rapidly to 14 D in simulated water at 300 K as the water reorganized to solvate the excited-state dipole moment, and the excited-state dipole moment in turn changed in response to the reaction field due to the water. A common theme in all of these computations is the large change in the charge distribution of the ^1L_a state that occurs during the excited-state lifetime in polar solvents. The magnitude of these changes illustrates the displaced nature of the ^1L_a transition and the hazards present in assuming that photophysical properties are independent of time and environment (as is assumed in the classical solvent shift relations.)

Inhomogeneous effects and solvent dependence

The Stark lineshape data in this work are analyzed under the assumption that the electrooptic properties of the molecule are not inhomogeneously distributed, or more precisely that the width of the distribution in a parameter is small compared with the magnitude of the parameter. The Stark signal is quadratic in $|\Delta\vec{\mu}|$ and $|\Delta\alpha|$, so the quantities determined are actually the square root of the ensemble average of the square of the quantity. For example, if $|\Delta\vec{\mu}|$ is characterized by a gaussian distribution with width σ and center value $|\Delta\vec{\mu}_0|$ the measured value is given by

$$\sqrt{\langle|\Delta\vec{\mu}|^2\rangle} = \frac{\int_{-\infty}^{\infty} |\Delta\vec{\mu}|^2 e^{-(|\Delta\vec{\mu}|-|\Delta\vec{\mu}_0|)^2/\sigma^2}}{\int_{-\infty}^{\infty} e^{-(|\Delta\vec{\mu}|-|\Delta\vec{\mu}_0|)^2/\sigma^2}} = \sqrt{\sigma^2 + |\Delta\vec{\mu}_0|^2} \tag{12}$$

so

$$\frac{\sqrt{\langle|\Delta\vec{\mu}|^2\rangle}}{\langle|\Delta\vec{\mu}|\rangle} = \frac{\sqrt{\sigma^2 + |\Delta\vec{\mu}_0|^2}}{|\Delta\vec{\mu}_0|} \tag{13}$$

where angle brackets denote an ensemble average. For instance, if $|\Delta\vec{\mu}_0|$ is 5 D and σ is 2 D, the measured value would be 5.39 D.

If there is a correlation between the value of an electrooptic parameter and the transition energy of a chromophore, the measured value will also depend on the region of the (inhomogeneously broadened) spectrum that is analyzed (Demchenko and Ladokhin, 1988). An interesting aspect of recent condensed-phase electronic structure calculations is the possibility of evaluating such correlations. Large variations in the ^1L_a dipole moment were predicted in several of the studies described above (Muiño et al., 1992; K. Krogh-Jespersen, personal communication), and in one of them (Muiño et el., 1992) a correlation was predicted, with red-absorbing solvent configurations characterized by larger excited-state dipole moments. Because we focus on the red part (although not the extreme low-energy tail that is usually the subject of "red-edge effect" investigations) of the absorption band, this experiment may be sensitive to this bias (Demchenko and Ladokhin, 1988). However, because an entire vibronic maximum is analyzed for each transition, a width of the order of the inhomogeneous linewidth is included in the analysis, and any bias must be correspondingly small. An experimental approach to the correlation of electrooptic parameters with transition energy is provided by the combination of electric field effects with line-narrowing spectroscopy (Meixner et al., 1992; Altmann et al., 1992). The most directly relevant of the available studies is that of Vauthey et al. (1993). For highly polar dyes in highly polar polymer matrices, a substantial wavelength dependence to the amplitude and lineshape of the electric field effect was observed. The lineshape changes indicated that the angle between $\Delta\vec{\mu}$ and $\vec{m}$ changed as a function of wavelength. The data were interpreted as a rotation of $\Delta\vec{\mu}$ brought about by changing relative contributions of "intrinsic" and matrix-induced difference dipole moments to $\Delta\vec{\mu}$, but we note that rotation of the transition moment due to vibronic coupling (see above) would provide an alternative mechanism.

The values of $|\Delta\vec{\mu}|$ recovered for both transitions for NATA in EtOH, NATA in glycerol/water, and mellitin are identical within the errors despite the rather large changes in 0–0 transition energies and inhomogeneous linewidths seen in Figs. 2 and 4. The Stark spectra in Fig. 3 reflect the differences in absorption lineshapes but are otherwise identical. The solvent-independence of the electrooptic properties is not consistent with significant inhomogeneous distortion of the recovered parameters. If the electrooptic properties are independent of solvent, they should be correspondingly insensitive to different local structures within the same solvent. It is interesting to note that the sample in the least polar solvent, NATA in EtOH, has the most redshifted ^1L_a and ^1L_b absorbance maxima, in contrast to the continuum electrostatic prediction. The ^1L_a linewidths, however, do follow the expected trends with solvent polarity.

Resolution of the ^1L_a and ^1L_b transitions

The decomposition of the ^1L_a and ^1L_b transitions in this work differs from that performed by Valeur and Weber (1977) in that the decomposed spectra were required to fit the Stark spectrum. Since this constraint was present, it was not necessary to assume a value for the limiting anisotropy of either transition, and these were left as free parameters in the fit. In the case of NATA and melittin, the assumption that the relatively flat region in the low-energy tail of the excitation anisotropy spectrum represents nearly pure ^1L_a absorption was born out by the fitting. The limiting anisotropy determined for the ^1L_a transition is less than the theoretical limiting value of 0.4 and indicates that the transition dipole moments on absorption and emission are not completely parallel. The values obtained (0.32–0.35) correspond to angles of 17–21°. Such rotations can derive from vibronic coupling (see above) or nuclear rearrangements during the excited-state lifetime.

Since the original experiment of Valeur and Weber (1977), two other experimental approaches to the decomposition of indole absorption spectra have been pursued. Albinsson and Nordén (1992) have measured linear dichroism spectra of indole and derivatives in stretched films, and Rehms and Callis (1987) have measured two-photon fluorescence excitation spectra. In addition, resolutions of a variety of derivatives have been performed by the fluorescence excitation anisotropy technique (Eftink et al., 1990). Of these, only the two-photon absorption measurements do not rely directly on wavelength-independent transition moment directions in order to measure relative ^1L_a and ^1L_b oscillator strengths. However, two-photon and one-photon lineshapes need not be identical, so there is at present no unambiguous means of decomposing the total absorption over the entire band. Our observations suggest that the available resolutions may not be even qualitatively useful except in the region of the 0–0 bands. As the analysis of Stark spectra depends rather sensitively on the absorption lineshape, it is likely that the largest nonstatistical errors in this experiment are due to violations of the assumptions necessary in the absorption decomposition.

CONCLUSION

The most robust conclusion of this work is that $|\Delta\vec{\mu}|$ for the ^1L_a transition of the indole chromophore in NATA and melittin is about 6.0 D/*f*. The long-wavelength absorption tail is due entirely to this transition, and the Stark spectrum in this region is dominated by a second-derivative contribution from it. It is therefore impossible to reproduce the experimental data by any other choice of parameters. The other parameters given in Table 1 are accurate within the assumptions necessary to decompose the absorption spectrum, but do not have as unique a relationship to the Stark spectrum. It can be stated that the ^1L_b $|\Delta\vec{\mu}|$ cannot be much larger than the value given. The magnitude of the Stark effect is proportional to the inverse square of the linewidth of a gaussian transition. Given that the linewidth of the ^1L_b 0–0 transition is much narrower than that of ^1L_a, a larger $|\Delta\vec{\mu}|$ for ^1L_b would have a dramatic effect on the total Stark lineshape. The value of the ^1L_a $|\Delta\vec{\mu}|$ we obtain is larger than that calculated from

solvent shifts or predicted by some electronic structure calculations. A value of the local field correction $f > 1.5$ would be necessary to produce agreement with these calculated values. This value of f is possible, but would be at the upper end of the likely range (Oh et al., 1991).

These results affect the interpretation of tryptophan fluorescence properties in several ways. First, if it is accepted that the ^1L_a $|\Delta\vec{\mu}|$ on absorption is larger than has been appreciated, quantitative conclusions as to the polarity of the environment based on absorption shifts must be rescaled. The situation with regard to fluorescence shifts is less clear, because the dipole moment may change significantly during the excited-state lifetime. Second, the evidence presented here for wavelength-dependent transition moment directions of one or both states must be taken into account in the interpretation of anisotropy-based measurements of conformational mobilities of tryptophan residues. For example, a rapid anisotropy decay component in the total emission could arise from vibrational relaxation, because different vibronic transitions have different transition moment directions. Such a component could easily be misinterpreted as deriving from motions or ^1L_a–^1L_b state dynamics.

This work was supported in part by a grant from the National Institutes of Health D.W.P. was supported in part by a National Science Foundation predoctoral fellowship and by the Biophysics Training Grant at Stanford University.

REFERENCES

Albinsson, B., and B. Nordén. 1992. Excited state properties of the indole chromophore: electronic transition moment directions from linear dichroism measurements: effect of methyl and methoxy substituents. *J. Phys. Chem.* 96:6204–6212.

Albinsson, B., M. Kubista, B. Nordén, and E. W. Thulstrup. 1989. Near-ultraviolet electronic transitions of the tryptophan chromophore: linear dichroism, fluorescence anisotropy, and magnetic circular dichroism spectra of some indole derivatives. *J. Phys. Chem.* 93:6646–6654.

Albrecht, A. C. 1961. Polarizations and the assignments of transitions: the method of photoselection. *J. Mol. Spectro.* 6:84–108.

Altmann, R. B., I. Renge, I. Kador, and D. Haarer. 1992. Dipole moment differences of nonpolar dyes in polymeric matrices: stark effect and photochemical hole burning. I. *J. Chem. Phys.* 97(8):5316–5322.

Beechem, J. M., and L. Brand. 1985. Time-resolved fluorescence of proteins. *Annu. Rev. Biochem.* 54:43–71.

Böttcher, C. J. F. 1973. Theory of Electric Polarization, 2nd ed, Vol. 1. Elsevier Scientific Publishing Company, Amsterdam. 77.

Boxer, S. G. 1993. Photosynthetic reaction center spectroscopy and electron transfer dynamics in applied electric fields. *In* The Photosynthetic Reaction Center, Vol. II. J. Deisenhofer and J. R. Norris, editors. Academic Press, San Diego. 179–220.

Boxer, S. G., A. Kuki, K. A. Wright, B. Katz, and N. H. Xuong. 1982. Oriented properties of the chlorophylls: Electronic absorption spectroscopy of orthorhombic pyrochlolophyllide α-apomyoglobin single crystals. *Proc. Natl. Acad. Sci. USA.* 79:1121–1125.

Callis, P. R. 1991. Molecular orbital theory of the ^1L_a and ^1L_b states of indole. *J. Chem. Phys.* 95:4230–4240.

Chabalowski, C. F., D. R. Garmer, J. O. Jensen, and M. Krauss. 1993. Reaction field calculations of the spectral shifts of indole. *J. Phys. Chem.* 97:4608–4613.

Demchenko, A. P., and A. S. Ladokhin. 1988. Red-edge-excitation fluorescence spectroscopy of indole and tryptophan. *Eur. Biophys. J.* 15: 369–379.

Eftink, M. R., L. A. Selvidge, P. R. Callis, and A. A. Rehms. 1990. Photophysics of indole derivatives: experimental resolution of L_a and L_b transitions and comparison with theory. *J. Phys. Chem.* 94:3469–3479.

Gladchenko, L. F., and L. G. Pikulik. 1967. Determination of dipole moments of indole and tryptophan in excited states. *Zh. Prikl. Spektrosk.* 6:355–60.

Hill, N. E., W. E. Vaughan, A. H. Price, and M. Davies. 1969. Dielectric Properties and Molecular Behavior. Van Nostrand Reinhold Company Ltd., London. 16–23.

Lakowicz, J. R. 1983. Principles of Fluorescence Spectroscopy. Plenum Press, New York. 128.

Lami, H., and N. Glasser. 1985. Indole's solvatochromism revisited. *J. Chem. Phys.* 84:597–604.

Levy, R., J. D. Westbrook, D. Kitchen., and K. Krogh-Jespersen. 1991. Solvent effects on the adiabatic free energy difference between the ground and excited states of methylindole in water. *J. Phys. Chem.* 95:6756–6758.

Lippert, E. 1957. *Z. Electrochem.* 61:962.

Liptay, W. 1976. *Ber. Bunsen-Ges. Phys. Chem.* 80:207–217.

Mataga, N., Y. Torihashi, and K. Ezumi. 1964. Electronic structures of carbazole and indole and the solvent effects on the electronic spectra. *Theoret. Chim. Acta.* 2:158–167.

Mathies, R. A. 1974. Experimental and Theoretical Studies on the Excited Electronic States of Some Aromatic Hydrocarbons through Electric Field Perturbation and through Chemical Substituents (Ph.D. thesis, Cornell University). University Microfilms International, Ann Arbor, MI. 99–139.

Meixner, A. J., A. Renn, and U. P. Wild. 1992. Spectral hole-burning and Stark effect: a centrosymmetric molecule in polymers of different dielectric constants. *Chem. Phys. Lett.* 190:75–82.

Muiño, P. L., D. Harris, J. Berryhill, B. Hudson, and P. R. Callis. 1992. Simulation of solvent dynamics effects on the fluorescence of 3-methylindole in water. J. R. Lakowicz, editor. *Proc. SPIE.* 1640: 240–251.

Oh, D. H., M. Sano, and S. G. Boxer. 1991. Electroabsorption (Stark effect) spectroscopy of mono- and biruthenium charge-transfer complexes: measurements of changes in dipole moments and other electrooptic properties. *J. Am. Chem. Soc.* 113:6880–6890.

Press, W. H., W. T. Vetterling, S. A. Teukolsky, and B. P. Flannery. 1992. Numerical Recipes in Fortran, 2nd ed. Cambridge University Press, New York.

Rehms, A., and P. R. Callis. 1987. Resolution of L_a and L_b bands in methyl indoles by two-photon spectroscopy. *Chem. Phys. Lett.* 140:83–89.

Valeur, B., and G. Weber. 1977. Resolution of the fluorescence excitation spectrum of indole into the ^1L_a and ^1L_b excitation bands. *Photochem. Photbiol.* 25:441–444.

Vauthey, E., K. Holliday, C. Wei, A. Renn, and U. P. Wild. 1993. Stark effect and spectral hole-burning: solvation of organic dyes in polymers. *Chem. Phys.* 171:253–263.

Walker, M. S., T. W. Bednar, and R. Lumry. 1967. Exciplex studies. II. Indole and indole derivatives. *J. Chem. Phys.* 47:1020–1028.

Westbrook, J. D., R. M. Levy, and K. Krogh-Jespersen. 1992. Simulation of photophysical processes of indoles in solution. J. R. Lakowicz, editor. *Proc. SPIE.* 1640:10–19.